Effect of annealing temperature on the physical of nanostructured TiO_2 films prepared by sol-gel method

A. A. Abdul Razaq[a], F. H. Jasim[b], S. S. Chiad[b], F. A. Jasim[a,*], Z. S. A. Mosa[c], Y. H. Kadhim[d]
[a]*Department of Physics, College of Science, Mustansiriyah University, Iraq*
[b]*Department of Physics, College of Education, Mustansiriyah University, Iraq*
[c]*Department of Pharmacy, Al-Manara College for Medical Science, Iraq*
[d]*Department of Optics Techniques, Al-Mustaqbal University College, Babylon, Iraq*

This study uses glass substrates to create nanostructured TiO_2 thin films employing Sol-Gel method. Afterwards, TiO_2 films are annealed in air for two hours at (400, 450, and 500) °C. The XRD tests demonstrate that all films are tetragonal polycrystalline and have orientations equal to those described in the literature. These findings suggest that when the annealing temperature rises, grain size increases. As the annealing temperature is raised, the Full Width at Half Maximum (FWHM) reduces from 0.57° to 0.0.51°, and the dislocation density drops from 45.22 to 39.22.18 nm, respectively. AFM has examined the thin films' surface morphology. The films formed using this method have good crystalline and homogenous surfaces, according to AFM tests. With an increase in annealing temperature, thin films' average particle size, average roughness, and Root Mean Square (RMS) value all drop. The films' optical characteristics. The transmission was over 97% decreased with increasing annealing temperatures. It is found that the band gap decreases from 3.42 to 3.3 eV with increasing annealing temperature. Between 300 and 900 nm, the films' refractive indices range from 2.89 to 2.2.76. With higher annealing temperatures, the films' extinction coefficients fall.

(Received November 24, 2023; Accepted March 5, 2024)

Keywords: Titanium oxide, Thin films, Sol-gel method, XRD, AFM, Optical and band gap

1. Introduction

The fabrication of oxide nanomaterials, including nanoparticles, nanotubes, nanofibers, nanorods, and nanolayers has significantly advanced nanotechnology in recent years. These materials have unique physical and chemical properties unheard of in ordinary materials. Due to their widespread availability and ease of use, simple materials like TiO_2, Al_2O_3, ZnO, SiO_2, and Bi_2O_3 [6] interest scientists. For more than 20 years, TiO_2 was one of the most extensively researched and utilized oxides. TiO2 is highly sought after by industry and science because of its many applications in various sectors, including chemical, electrical, pharmaceutical, architectural, and cosmetic. Its outstanding catalytic capabilities, reasonable cost, strong physical and chemical stability, and non-toxic composition are the reasons for its popularity in a scientific investigation [7]. At the moment, one of the most intriguing photochemical materials is this one. [8]. In nature, titanium dioxide can be found in three polymorphic minerals: rutile, reasonably unusual rhombic brucite, and the most frequent, tetragonal anatase. Each polymorphic form has a different band gap, which is 2.96 eV for brucite, 3.03 eV for rutile, and 3.32 eV for anatase [2]. TiO_2 can be used as self-cleaning layers ,solar cells [9,10]. TiO_2 thin films can be synthesized using various techniques: ion beam [11], anodic [12], PECVD [13], CVD [14], PLD [15], Plasma spray [16], including thermal [17], Spray Pyrolysis Technique [18-20]. RF sputtering method [21, 22] and sol–gel method [23-24]. The sol-gel process, can be applied in coating large surfaces, inexpensive,

* Corresponding author: farah.abdulrazzaq.j@gmail.com
https://doi.org/10.15251/JOR.2024.202.131

and easily the homogeneity of the layer's structure can be controlled [25–28]. In this study, we focus on preparation of nanostrucured TiO_2 thin films, and examine how the annealing temperature affects the optical, surface morphological, and structural characteristics of TiO_2 films.

2. Experimental

Titanium tetraisopropoxide [$Cl_2H_28O_4Ti$] 0.1M solution is dissolved in methanol to prepare the sol. The cloudy solution was made clear by stirring one drop of HCL and 1 drop of H_2O with a 0.25 ml micropipette. After that, the entire solution was placed in a secure area to age for two days. The solution is ready to create TiO_2 films utilizing spin coating on a glass substrate of 2.5 x 7 cm^2. The 140 Volt spinning rate was maintained. The wet films were annealed for one hour after being dried at 75 ^oC for 10 minutes. The procedure was repeated to get the film's usable thickness of 10 nm. Films with multiple layers were pre-annealed at 400°C and then post-annealed for an hour at 450°C and 500°C. Using CuK radiation with a wavelength of 0.15406 nm, an X-ray diffractometer (XRD, SEIFERT) was used to analyze the structural characteristics of thin films (AFM, SPA 400). The transmission spectra were captured using a UV-VIS Spectrophotometer (Systronics Double Beam Spectro-Photometer Model 2202).

3. Results and discussions

The X-ray diffraction patterns for films produced of the polycrystalline material TiO_2 are shown in Figure 1. (3) Several peaks with diffraction angles of 25.26°, 48.43°, and 62.61° are observed in TiO_2 thin films. They are, respectively, attributed to the (101), (200), and (204) planes. The standard TiO_2 X-ray diffraction data file [No. 21-1272] JCPDS prevalent is consistent with these findings. Nonetheless, TiO_2 thin films have been found to have the hexagonal favoured orientation (101), as in our instance. [29].
The average grain size (*D*), which can be estimated via Scherrer's formula [30-32]:

$$D = \frac{K\lambda}{\beta cos\theta} \tag{1}$$

K = 0.89, λ is the wavelength of x-rays, β is FWHM, and θ is the Bragg angle. *D* was raised from 14.87 nm to 15.96 nm with an increase in annealing temperature (T_a) ,Which agree with [29], as shown in Table. The surface morphology is fine and regular with spherical nanoparticles (1).

This Dislocation density (δ) can be calculated from the formula [33-35]:

$$\delta = \frac{1}{D^2} \tag{2}$$

The dislocation density is found to be 45.22, 43.96 and 39.22 as T_a rise.

This strain (Ɛ) can be calculated from Eq.3[36-38]:

$$\varepsilon = \frac{\beta cos\theta}{4} \tag{3}$$

The strain is discovered to be 24.26, 22.99, and 21.75 annealed, as T_a rise. Figure (2) shows the prepared films' FWHM, *D*, δ, and strain. *D* and other factors have an inverse relation.

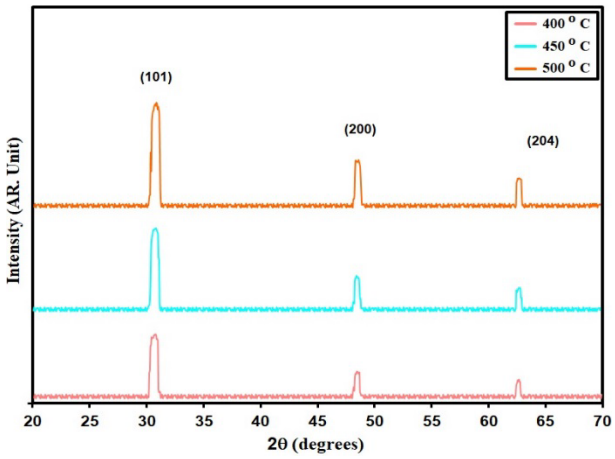

Fig. 1. XRD pattern of the intended films.

Table 1. Structural coefficient, D and optical bandgap of grown films.

Sample (°C)	2 θ (°)	(hkl) Plane	FWHM (°)	Optical bandgap (eV)	Grain size (nm)	Dislocations density ($\times 10^{14}$) (lines/m^2)	Strain ($\times 10^{-4}$)
400	25.26	101	0.57	3.42	14.87	45.22	24.26
450	25.22	101	0.54	3.37	15.08	43.96	22.99
500	25.19	101	0.51	3.33	15.96	39.22	21.75

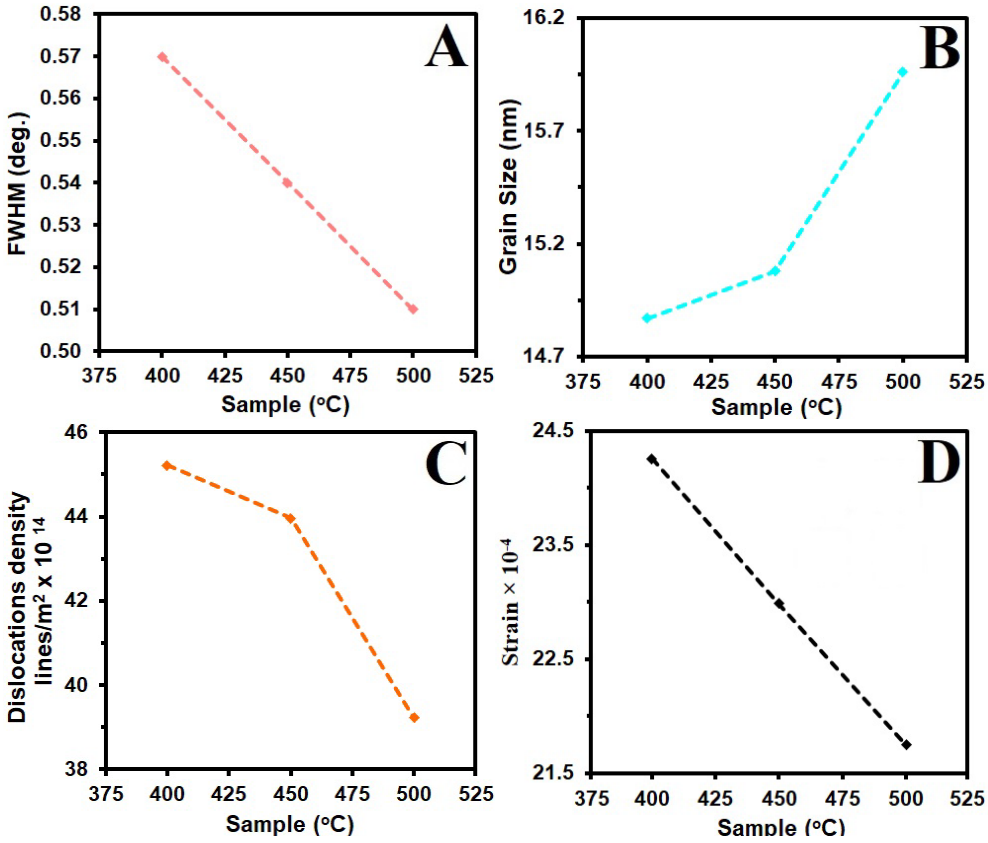

Fig. 2. FWHM (a) D (b) δ (c) ε (d) of the as-deposited TiO_2 thin.

4. Topography surface analysis

Figure 3 displays the AFM images after annealing them at (400, 450, and 500) °C. The grains are distributed somewhat equally over the scanning zone (10 × 10 m), as seen in Figures (3). The three-dimensional properties at (400, 450, and 500) °C are displayed in Figure 3 (A1, A2, and A3). As can be seen from the AFM micrographs, the grains are consistently round. According to Table 2, the average particle size (P_{av}) of a TiO_2 film after annealing was arranged to be between 70.4 and 33.4 nm, with the average surface roughness Ra falling between 6.31 and 2.77 nm and the root mean square (rms) falling between 9.10 and 2.78 nm. Figure (3) and Table 2 provide AFM parameter (P_{AFM}) values for the grown films.

Table 2. PAFM of the grown films.

Sample (^oC)	P_{av} (nm)	R_a (nm)	RMS (nm)
400	70.4	6.31	9.10
450	50.3	3.42	7.93
500	33.4	2.77	2.78

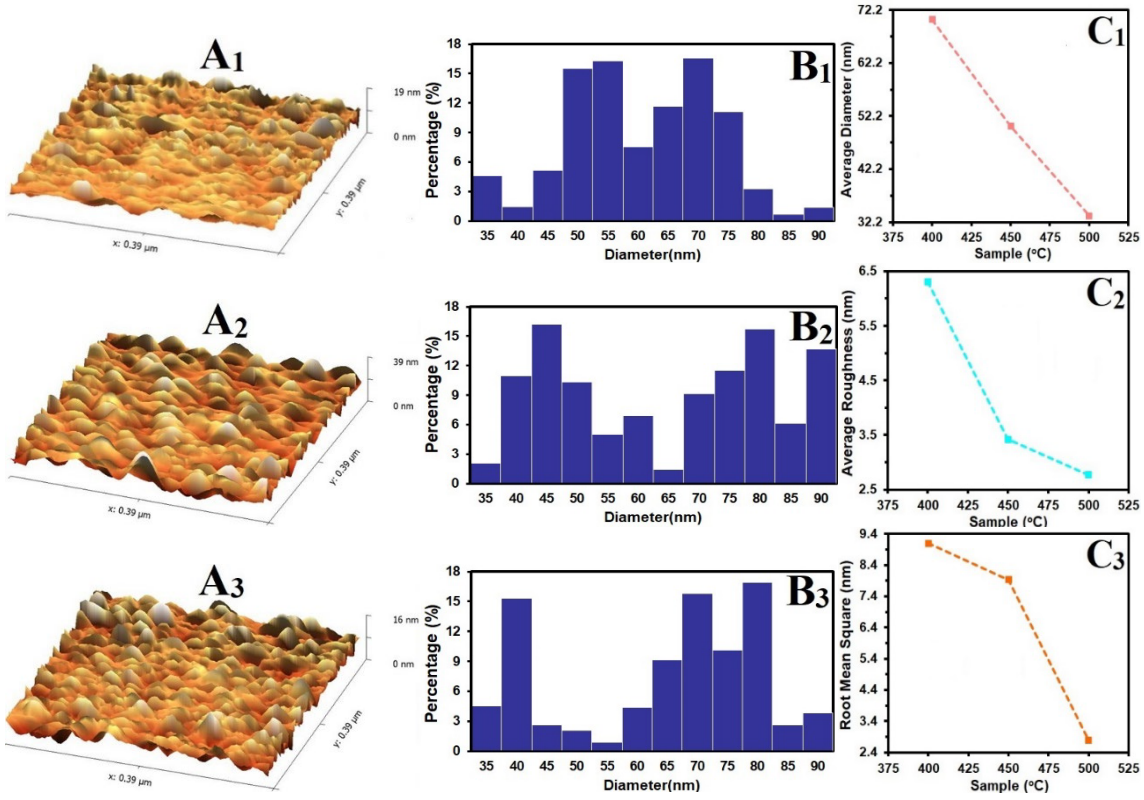

Fig.3. AFM information of deposit films.

5. Optical properties analysis

According to Fig., T_a significantly influences the optical transmittance (T) measurements of the TiO_2 films (4). It is discovered that films have a near-infrared transparency of nearly 97%. It has been found that T decreases with increasing the T_a for all films examined; this is due to the film surface becoming rougher and the surface scattering of light becoming more pronounced as a result of increasing columnar growth with needle- and rod-like shapes [36,37]. Higher-temperature

annealed TiO_2 films exhibit decreased transmittance. Since annealing increases the roughness of a film's surface, it scatters light [39].

The measured absorbance (A) of TiO_2 thin films is related to T by [40-41]:

$$A = \log\left(\frac{1}{T}\right) = \left(\frac{I}{I_o}\right) \tag{4}$$

where (I) is the transmitted light and (I_o) is the incident light. T_a affects A, as seen in Fig (5). Further analysis indicates A increases with an increase in T_a. The increase in particle sizes is responsible for this. The TiO_2 film annealed at 500 ^oC exhibits the highest absorption. The absorption edges exhibit a slight red shift as T_a rises. The absorption edge may redshift for a variety of reasons. One is that the absorption edge may redshift due to bigger crystals [42].

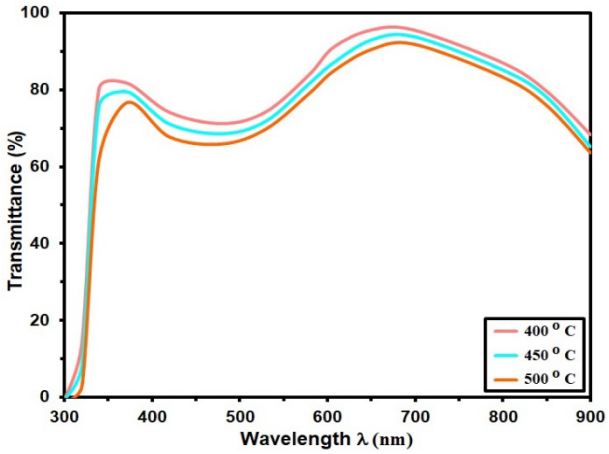

Fig. 4. T of grown films.

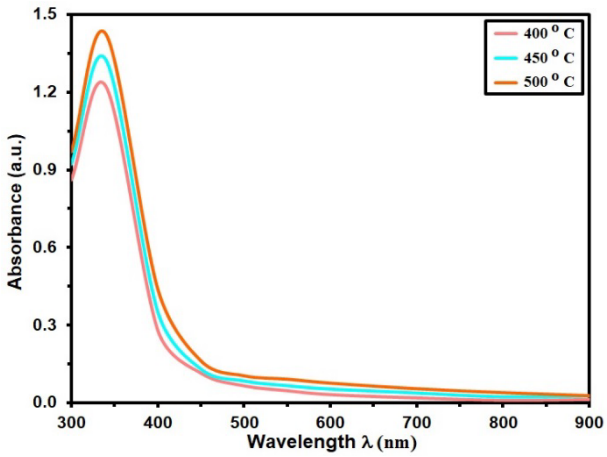

Fig. 5. Absorbance with wavelength of the as-deposited TiO_2 thin films.

Equation 5 [43, 42] was used to determine the absorption coefficient (α) as shown in Fig. (6):

$$\alpha = (2.303 \times A)/t \tag{5}$$

where (t) is film thickness, since α is inversely proportional to the transmittance, it increases strongly in the UV range and progressively decreases (Fig. 6). As the annealing temperature rises,

the absorption coefficient rises as well, and its value is more than (10^4 cm^{-1}). This is related to increased grain size, and the light scattering effect may explain its high surface roughness. [4].

The analysis was conducted using the method described in [27, 28] to ascertain the energy gaps in the materials created. The following is assumed to be the dependence of the substance under investigation's of α on radiation: [45-46]

$$(\alpha h\nu) = A\left(h\nu - E_g\right)^n \tag{6}$$

where E_g is the band gap, A is energy independent constant, (hν) is photon energy, n=1/2. The conditions for film deposition and its preparation procedure, which impact the crystalline structure, determine the energy gap value. [47]. The cause for the variance in the energy gap is the variation in the structural characteristics and other changes. Fig. 7 shows that as T_a is raised, the allowable E_g decreases from 3.3.42 to 3.3 eV. They are well-concordant with those reported for TiO_2 thin films made using other methods. [14].

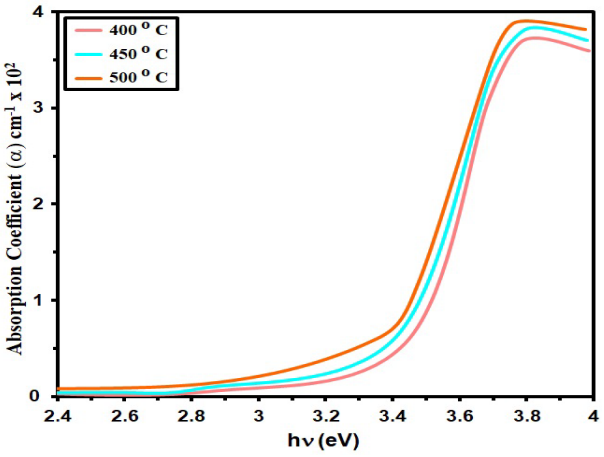

Fig. 6. α of the as-deposited TiO_2 films.

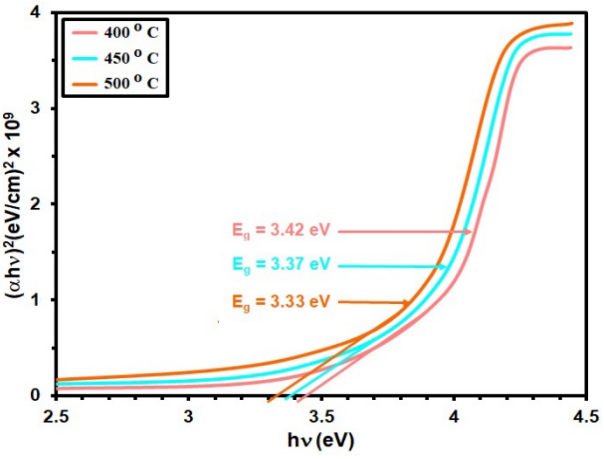

Fig. 7. (αhν)2 of the as-deposited TiO_2 films.

Equation (7) relates the extinction coefficient (K) [48-49]:

$$k = \frac{\alpha\lambda}{4\pi} \tag{7}$$

where (λ) is the wavelength of the incident radiation, so (k) can be measured by using the previous relation. Figure 1 displays k curves for TiO_2 films grown and annealed (8). Extinction coefficient has the same behavior as α due to their prior relationship, but the k declines as annealing temperature increases [50, 51].

Equation 8 is used to determine the thin films of TiO_2's refractive indices (n) [52,53]:

$$n = \left(\frac{1+R}{1-R}\right) + \sqrt{\frac{4R}{(1-R)^2} - k^2} \tag{8}$$

The fluctuation in n in the (350-900 nm) wavelength range is depicted in Fig. (9). n in the visible/near-infrared range increases as T_a rises. n also drops in the visual region as the wavelength rises [9]. This pattern demonstrates an increase in n value with greater annealing temperature [54]. The increased packing density and T_a impact the films' morphology (change in crystalline structure), which is responsible for the change in n. n values range from 2.1 to 2.8 for films with various T_a [55] According to a few researchers, n of deposited or annealed TiO_2 films ranges from 2.1 to 2.9, and annealing treatment causes n to drop because it increases crystallization. [56].

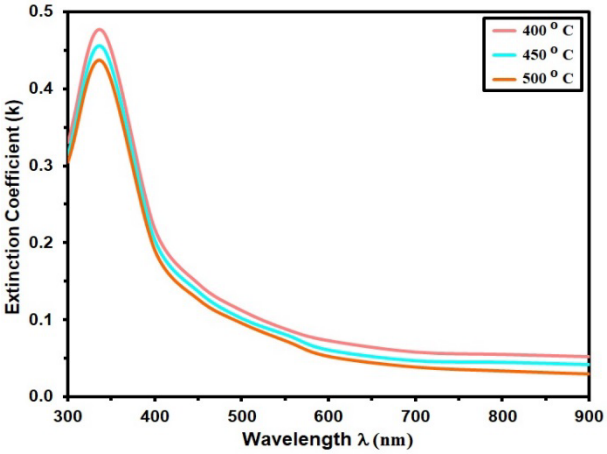

Fig. 8. k of the as-deposited films.

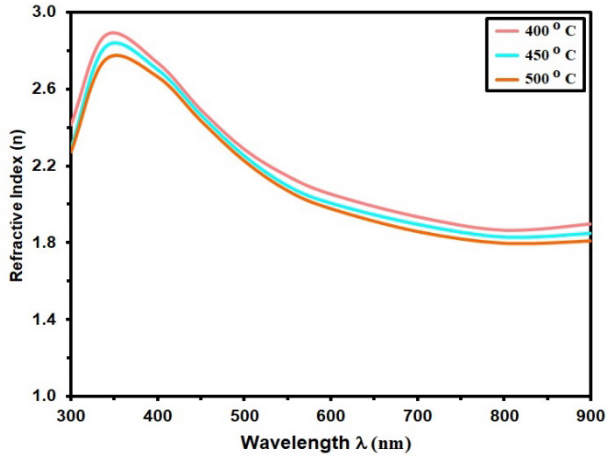

Fig. 9. n of the as-deposited TiO2 thin films.

6. Conclusion

Sol-gel creates nanostructured TiO_2 thin films. A polycrystalline structure with high peak intensities in the (101), (200), and (211) planes is seen in the TiO_2 films, and the grain size increases as T_a is elevated from (400 to 500 ^oC), but the dislocation density and strain decreases. According to the AFM data, the average particle size reduces from 70.4 nm to 33.4 nm as the annealing temperature rises from 400 to 500 °C. As T_a increases, the root mean square (RMS) similarly drops from 9.1 to 2.78 nm. The average transmittance is around 97% in the near-infrared range. The least transmitting of all the films is the one that has been annealed at 500 °C. Still, because optical absorptance is vital at short wavelengths, the film is suitable for a detector in the ultraviolet region. TiO_2 sheets have an α of approximately ($>10^4$ cm^{-1}), meaning that as photon energy increases, so does α. Also, the optical characteristics of thin films made of TiO_2 demonstrate that direct transition was possible. The optical band gap, n , and k, all drop as the annealing temperature is raised for all films.

Acknowledgements

This work was supported and financed by Mustansiriyah University (www. uomustansiriyah.edu.iq).

References

[1] Y. Qian, J. Du, D. J. Kang, Microporous Mesoporous Mater, 273, 148–155 (2019); https://doi.org/10.1016/j.micromeso.2018.06.056.

[1] J.-i Fujisawa, Chem. Phys. Lett., 739, 136974 (2020); https://doi.org/10.1016/j.cplett.2019.136974.

[3] J. Mohapatra, M. Xing, J. Elkins, J. Ping Liu, J. Alloys Compd., 824, 153874 (2020); https://doi.org/10.1016/j.jallcom.2020.153874.

[4] G. B. Soares, R.A.P. Ribeiro, S.R. de Lazaro, C. Ribeiro, N. RSC Adv., 6, 89687–89698 (2016); https://doi.org/10.1039/C6RA15825K.

[5] S. S. Chiad, T. H. Mubarak, International Journal of Nanoelectronics and Materials, 13 (2), 221-232 (2020).

[6] A. A. Khadayeir, E. S. Hassan, S. S. Chiad, N. F. Habubi, K. H. Abass, M. H. Rahid, T. H. Mubarak, M. O. Dawod, and I.A. Al-Baidhany, Journal of Physics: Conference Series 1234 (1), 012014, (2019); https://doi.1088/1742-6596/1234/1/012014

[7] N. Y. Ahmed, B. A. Bader, M. Y. Slewa, N. F. Habubi, S. S. Chiad, NeuroQuantology, 18(6), 55-60 (2020); https://doi.org/10.14704/nq.2020.18.6.NQ20183

[8] G. Sadanandam, X. Luo, X. Chen, Y. Bao, K. P. Homewood, Y. Gao, Appl. Surf. Sci., 541, 148687 (2021); https://doi.org/10.1016/j.apsusc.2020.148687.

[9] A. Y. Madkhli, W. Shirbeeny, Physica B Condens. Matter, 597, 412414 (2020); https://doi.org/10.1016/j.physb.2020.412414.

[10] K. Pubby, K. V. Babu, S. B. Narang, Mater. Sci. Eng., B, 225, 114513 (2020); https://doi.org/10.1016/j.mseb.2020.114513.

[11] C.Yang, H. Fan, Y. Xi, J. Chen, Z. Li, Applied Surface Science, 254, 2685–2689 (2008); https://doi.org/10.1016/j.apsusc.2007.10.006

[12] M.R. Kozlowski, P.S. Tyler, W.H. Smyrl, R.T. AtanasokiJ. Electrochem. Soc. 136, 442-450(1989); https://doi.org/10.1016/0022-0728(87)85243-9

[13] W. Yang, C. A. Wolden Thin Solid Films, 515, 1708–1713 (2006); https://doi.org/10.1016/j.tsf.2006.06.010

[14] V. G. Besserguenev, R. J. F. Pereira, M. C. Mateus, I. V. Khmelinskii, R. C. Nicula, E. Burkel, International Journal of Photoenergy, 5, 99-105 (2003); https://doi.org/10.1155/S1110662X03000205
[15] N. Inoue, H. Yuasa, M. Okoshi. Applied Surface Science, 197–198, 393–397 (2002); https://doi.org/10.1016/S0169-4332(02)00347-1
[16] A. Sharma, A. Gouldstone, S. Sampath, R. J. Gambino, J. Appl. Phys., 100, 114906 (2006); https://doi.org/10.1063/1.2382456
[17] G.-J. Yang, C.-J. Li, F. Han, and X.-C. Huang, J. Vac. Sci. Technol. Bhttps 22, 2364 (2004); https://doi.org/10.1116/1.1788679
[18] H. P. Deshmukh, P. S. Shinde, P. S. Patil, Materials Science and Engineering: B, 130 (1-3), 220–227 (2006); https://doi.org/10.1016/j.mseb.2006.03.016
[19] V. Sivaranjan ,P. Deepa, P. Philominathan, International Journal of Thin films Science and Technology, No. 2, 125-131 (2015); http://dx.doi.org/10.12785/ijtfst/040210
[20] I. Joseph Panneerdoss, S. Johnson Jeyakumar, M. Jothibas, International Journal Of Engineering and Science, 4 (11), , PP15-20 (2014); https://doi.org/10.1016/j.surfin.2014.100482
[21] C. Ho Heo, S.Lee, J. Boo, Thin Solid Films, 475, 183– 188 (2005); https://doi.org/10.1016/j.tsf.2004.08.033
[22] H. Pulker, G. Paesold and E. Ritter, Appl. Opt., 15, 2986-2991(1976); https://doi.org/10.1364/AO.15.002986
[23] J. Y. Kim, D. W. Kim, H. S. Jung, K. S. Hong, Jpn. J. Appl. Phys. 44, 6148-6151(2005); https://doi.org/10.1143/JJAP.44.6148
[24] M. Momeni, H. Saghafian, F. Golestani-Fard, N.Barati, and A.Khanahmadi, *Applied Surface Science* 392 (15), 80-87 (2017); https://doi.org/10.1016/j.apsusc.2016.08.165
[25] E. H. Hadi, M. A. Abbsa, A. A. Khadayeir, Z. M. Abood, N. F. Habubi, and S.S. Chiad, Journal of Physics: Conference Series, 1664 (1), 012069 (2020); https://doi.org/ 10.1088/1742-6596/1664/1/012069
[26] M. S. Othman, K. A. Mishjil, H. G. Rashid, S. S. Chiad, N. F. Habubi, I. A. Al-Baidhany, Journal of Materials Science: Materials in Electronics, 31(11), 9037-9043 (2020); https://doi.org/10.1007/s10854-020-03437-0
[27] E. H. Hadi, D. A. Sabur, S. S. Chiad, N. F. Habubi, K., Abass, Journal of Green Engineering, 10 (10), 8390-8400 (2020); https://doi.org/10.1063/5.0095169
[28] Hassan, E.S., Mubarak, T.H., Chiad, S.S., Habubi, N.F., Khadayeir, A.A., Dawood, M.O., Al-Baidhany, I. A. , Journal of Physics: Conference Series, 1294(2), 022008 (2019); https://doi.1088/1742-6596/1294/2/022008
[29] N. Suriyachai, S. Chuangchote, N. Laosiripojana, V. Champreda, ACS Omega, 5, 20373 (2020); https://doi.org/10.1021/acsomega.0c02334.
[30] N. N. Jandow, M. S. Othman, N. F.Habubi, S. S. Chiad, K. A. Mishjil, I. A. Al-Baidhany, Materials Research Express, 6 (11), (2020); https://doi.org/10.1088/2053-1591/ab4af8
[31] E. S. Hassan, K. Y. Qader, E. H. Hadi, S. S. Chiad, N. F. Habubi, K. H. Abass, Nano Biomedicine and Engineering, 12(3), pp. 205-213 (2020); https://doi.org/10.5101/nbe.v12i3.p205-213
[32] M. D. Sakhil, Z. M. Shaban, K. S. Sharba, N. F. Habub, K. H. Abass, S. S. Chiad, A. S. Alkelaby, NeuroQuantology, 18 (5), 56-61 (2020); https://doi.org/10.14704/nq.2020.18.5.NQ20168
[33] N. Y. Ahmed, B. A. Bader, M. Y. Slewa, N. F. Habubi, S. S. Chiad, NeuroQuantology, 18(6), 55-60 (2020); https://doi.org/10.1016/j.jlumin.2021.118221
[34] Khadayeir, A. A., Hassan, E. S., Mubarak, T. H., Chiad, S.S., Habubi, N. F., Dawood, M.O., Al-Baidhany, I. A., Journal of Physics: Conference Series, 1294 (2) 022009(2019); https://doi.1088/1742-6596/1294/2/022009
[35] A. J. Ghazai, O. M. Abdulmunem, K. Y. Qader, S. S. Chiad, N. F. Habubi, AIP Conference Proceedings 2213 (1), 020101 (2020); https://doi.org/10.1063/5.0000158
[36] H. A. Hussin, R. S. Al-Hasnawy, R. I. Jasim, N. F. Habubi, S. S. Chiad, Journal of Green Engineering, 10(9), 7018-7028 (2020); https://doi.org/10.1088/1742-6596/1999/1/012063

[37] S. S. Chiad, H. A. Noor, O. M. Abdulmunem, N. F. Habubi, M. Jadan, J. S. Addasi, Journal of Ovonic Research, 16 (1), 35-40 (2020). https://doi.org/10.15251/JOR.2020.161.35
[38] H. T. Salloom, E. H. Hadi, N. F. Habubi, S. S. Chiad, M. Jadan, J. S. Addasi, Digest Journal of Nanomaterials and Biostructures, 15 (4), 189-1195 (2020); https://doi.org/10.15251/DJNB.2020.154.1189
[39] J. Yu, J. Zou, P. Xu, Q. He, J. Clean. Prod. 251, 119744 (2020); https://doi.org/10.1016/j.jclepro.2019.119744.
[40] R. S Ali, N. A. H. Al Aaraji, E. H. Hadi, N. F. Habubi, S. S. Chiad, Journal of Nanostructuresthis link is disabled, 10(4), 810–816 (2020); https://doi: 10.22052/jns.2020.04.014
[41] A. A. Khadayeir, R. I. Jasim, S. H. Jumaah, N. F, Habubi, S. S. Chiad, Journal of Physics: Conference Series,1664 (1) (2020); https://doi.org/10.1088/1742-6596/1664/1/012009
[42] Z. Wu, D. Yuan, S. Lin, W. Guo, D. Zhan, L. Sun, C. Lin,. Int. J. Hydrog. Energy, 45, 32012-32021 (2020);. https://doi.org/10.1016/j.ijhydene.2020.08.258.
[43] S. S Chiad,, A. S. Alkelaby, K. S. Sharba,, Journal of Global Pharma Technology, 11 (7), 662-665, (2020); https://doi.org/10.1021/acscatal.1c01666
[44] Chiad, S.S., Noor, H.A., Abdulmunem, O.M., Habubi, N.F., Journal of Physics: Conference Series 1362(1), 012115 (2019); https://doi.org/10.1088/1742-6596/1362/1/012115
[45] R. S. Ali, M. K. Mohammed, A. A. Khadayeir, Z. M. Abood, N. F. Habubi and S. S. Chiad, Journal of Physics: Conference Series, 1664 (1), 012016 (2020); https://doi:10.1088/1742-6596/1664/1/012016
[46] A. S. Al Rawas, M. Y. Slewa, B. A. Bader, N. F. Habubi, S. S. Chiad, Journal of Green Engineering,10 (9), 7141-7153 (2020); https://doi.org/10.1021/acsami.1c00304
[47] N. Mozaffari, S. M. Elahi, S. S. Parhizgar, Int. J. Thermophys. 40, 67 (2019); https://doi.org/10.1007/s10765-019-2533-1.
[48] K. Y. Qader, R. . Ghazi, A. M. Jabbar, K. H. Abass, S. S. Chiad, Journal of Green Engineering, 10 (10), 7387-7398, 2020. https://doi.org/10.1016/j.jece.2020.104011
[49] R. S. Ali, H. S. Rasheed, N. F. Habubi, S.S. Chiad, Lettersthis link is disabled, 20 (1), 63–72 (2023; https://doi.org/10.15251/CL.2023.201.6
[50] T. Hoseinzadeh, S. Solaymani, S. Kulesza, A. Achour, Z. Ghorannevis,, Ş. Ţălu, M. Bramowicz, M. Ghoranneviss, S. Rezaee, A. Boochani, N. Mozaffari., J. Electroanal. Chem., 830–831, 80-87 (2018); https://doi.org/10.1016/j.jelechem.2018.10.037.
[51] A. Ghazai, K. Qader, N. F. Hbubi, S. S. Chiad, O. Abdulmunem, IOP Conference Series: Materials Science and Engineering, 870 (1), 012027 (2020); https://doi.org/ 10.1088/1757-899X/870/1/012027
[52] B. A. Bader, S. K. Muhammad, A. M. Jabbar, K. H. Abass, S. S. Chiad, N. F. Habubi, J. Nanostruct, 10(4): 744-750, (2020); https://doi.org/ 10.22052/JNS.2020.04.007
[53] O. M. Abdulmunem, A. M. Jabbar, S. K. Muhammad, M. O. Dawood, S. S. Chiad, N. F. Habubi, Journal of Physics: Conference Series,1660 (1), 012055 (2020); https://doi.org/ 10.1088/1742-6596/1660/1/012055
[54] N. N. Jandow, N. F. Habubi, S. S. chiad, I. A. Al-Baidhany and M. A. Qaeed, International Journal of Nanoelectronics and Materials, 12 (1), 1-10 2019.
[55] M.O. Dawood, S.S. Chiad, A.J. Ghazai, N.F. Habubi, O.M. Abdulmunem, AIP Conference Proceedings 2213, 020102,(2020); https://doi.org/10.1063/5.0000136
[56] A. Chanda, S. R. Joshi, V. R. Akshay, S. Varma, J. Singh, M. Vasundhara, P. Shukla, Appl. Surf. Sci., 536, 147830 (2021); https://doi.org/10.1016/j.apsusc.2020.147830.
[42] G. Sadanandam, K. Lalitha, V. D. Kumari, M. V. Shankarb, M. Subrahmanyam, Int. J. Hydrog. Energy, 38, 9655-9664 (2013); https://doi.org/10.1016/j.ijhydene.2013.05.116.
[43] M. M. Momenin, Y. Ghayeb, Ceram. Int., 42, 7014-7022 (2016); https://doi.org/10.1016/j.ceramint.2016.01.089.
[44] R. S. Dubey, S. Singh, Results Phys., 7, 1283-1288 (2017); https://doi.org/10.1016/j.rinp.2017.03.014.
[45] T. K. Maity, S. L.Sharma, Bull. Mater. Sci., 31 (6) 841–846 (2008);

https://doi.org/10.1007/s12034-008-0134-x
[46] X. Li, F. He, G. Liu, Y. Huang, C. Pan, C. Guo, Materials Letters, 67 369–372 (2012); https://doi.org/10.1016/j.matlet.2011.09.111
[47] X. He, C. P. Yang, G. L. Zhang, D. W. Shi, Q. A. Huang, H. B. Xiao, Y. Liu, R. Xiong, Mater. Des. 106, 74–80 (2016); https://doi.org/10.1016/j.matdes.2016.05.025.
[48] M. Hamadanian, A. Reisi-Vanani, A. Majedi, J. Iran. Chem. Soc., 7, 52–58 (2010); https://doi.org/10.1007/BF03246184.
[49] S. Mugundan, B. Rajamannan, G. Viruthagiri, N. Shanmugam, R. Gobi, P. Praveen, Appl. Nanosci. 5, 449–456 (2015); https://doi.org/10.1007/s13204-014-0337-y.
[50] Y. Ju, M. Wang, Y. Wang, S. Wang, C. Fu, Adv. Condens. Matter Phys., 2013, 5 (2013); https://doi.org/10.1155/2013/365475.
[51] A. Chanda, K. Rout, M. Vasundhara, S. R. Joshi, J. Singh, RSC Adv., 8, 10939–10947 (2018); https://doi.org/10.1039/C8RA00626A.
[52] Z. G. Hu, W. W. Li, J. D. Wu, J. Sun, Q. W Shu, X. X. Zhong, Z. Q. Zhu, J. H. Chu, Appl. Phys. Lett., 93, 181910 (2008); https://doi.org/10.1063/1.3021074.
[33] F. Mostaghni, Y. Abed, Mater. Sci.-Poland, 34, 534-539 (2016);
https://doi.org/10.1515/msp-2016-0071.
[53] M. Abushad, M. Arshad, S. Naseem, S. Khan. W. Husain, Mater. Chem. Phys. 256, 123641 (2020); https://doi.org/10.1016/j.matchemphys.2020.123641
[54] A. Boutlala, F. Bourfaa, M. Mahtili, A. Bouaballou, IOP Conf. Ser.: Mater. Sci. Eng., 108, 012048 (2016); https://doi.org/10.1088/1757-899X/108/1/012048.